Science and Technology
RMUTT Journal
Vol.7 No.2 (2017) : 153–167
www.sci.rmutt.ac.th/stj
Online ISSN 2229-1547

The Performance Analysis of Universal Inspection Registration for Video Multi-Frame Super Resolution Reconstruction Established on Stochastic Maximum A Posteriori Framework

Vorapoj Patanavijit

Assumption University of Thailand
E-mail: patanavijit@yahoo.com

Abstract

Traditionally, the classical Multi-frame Super Resolution Reconstruction (MSRR) schemes can be effectively implemented on the video with a simple shifting motion pattern because the conventional inspected model in video MSRR scheme is established on an ordinary registration. In this paper, the universal inspection registration (established on a fast affine block-based transform) has been proposed for handling with any real and complex inter-frame motion patterns therefore this the video MSRR cooperated with the proposed registration can be applied on any real and complex videos. Later, this paper mathematically presents the solution (or the refined SR image) of the video MSRR with the proposed registration under the regularization framework by using an optimized nonlinear programing technique. Using two tested video sequences such as Susie and Foreman with four noise models at several noise energy, the refined SR image products from experiments expose that the MSRR schemes with the proposed registration outperforms than the antecedent MSRR schemes with the an ordinary registration.

Keywords: SRR (Super-Resolution Reconstruction), DIR (Digital Image Reconstruction), DIP (Digital Image Processing), MAP (Maximum A Posteriori) Estimation, Registration

Received: June 10, 2016
Revised: October 24, 2017
Accepted: November 28, 2017

1. Antecedent Researched Tasks and Researched Problem

This division rehearses the antecedent research tasks from the registration perspective due to the reason that the grade of the refined SR image is contingent severely on the trustworthy of the inspection model; in fact, subpixel-level trustworthy in the nonisometric inter-frame motion pattern is demanded to achieve the expected progress. The ordinary MSRR schemes reviewed in [10, 11, 12, 14, 16, 25] are established on a simple inspection registration using globally or locally shifting motion pattern for handling with the effortless synthesized LR images [3, 23, 29] or real LR sequences with a shifting motion pattern [1, 27] because the ordinary MSRR schemes assume that these LR images or video are inspected at a satisfied temporal sampling frame rate. Like almost tested standard sequences (Carphone, Foreman, Mobile Calendar, Susie, etc.), the real LR images or LR video are often inspected by a real smart phone or real digital camera at a low temporal sampling frame rate wherefore these real LR images or LR video comprise of several complicated motion patterns instead of only simple shifting motion patterns. Consequently, the registration trustworthy is not sufficient for modeling these complicated motion patterns and the refined SR image products from the MSRR established on shifting motion pattern is degraded.

For enlarging the ordinary inspected model [3-8, 27] to nonisometric inter-frame pattern, so called affine inspection registration, the MSRR scheme [28] established on stochastic maximum a posteriori (MAP) framework with the enlarged inspected model was rehearsed in 2006. In 2007, the MSRR scheme [9] established on stochastic maximum a posteriori (MAP) framework with the more general inspected model (shifting motion pattern and rotational motion pattern) was rehearsed.

In order to conquer the above registration problem, which is insufficient temporal frame rate and cannot model these complicated motion patterns, this paper confers the video MSRR scheme established on stochastic maximum a posteriori framework with universal inspection registration [15] that is found on fast affine block-based transform [13]. The proposed universal inspection registration is not only a subpixel-level trustworthy in the nonisometric inter-frame motion pattern but the registration information is also estimated by a fast technique for attenuating the calculated time.

This article is partitioned into five main divisions as forthcoming. The first division rehearses antecedent researched tasks from registration perspective and, later, discusses the researched problems. The second division rehearses the stochastic impression of the MSRR problem formulation established on stochastic maximum a posteriori (MAP) framework with the ordinary registration and universal inspection registration. Next, the third division rehearses the video MSRR scheme established on stochastic maximum a posteriori framework with universal inspection registration for modeling these complicated motion patterns. Proving by simulating under four noise models at several noise energy levels on Susie and Foreman, copious refined SR image products are simulated for exposing that the MSRR schemes with the proposed universal inspection registration outperforms than the original MSRR schemes. Finally, the discussion and summary are rehearsed in the fifth division.

2. The Stochastic Impression of MSRR Problem Formulation of the Ordinary Registration and its Solution

In this division, we rehearse the MSRR problem, which is stochastically formulated by using the ordinary observation model (a simple shifting motion pattern) and, later, we rehearse the solution of MSRR problem, which is solved by using an optimized nonlinear programing technique.

2.1 The Ordinary Registration of MSRR Scheme

The inspected LR images or LR video are expounded as $\{\underline{\mathbf{Y}}_k\}$, which have the measurement as $N_1 \times N_2$, and artistic HR image is expounded as $\underline{\mathbf{X}}$, which have the measurement as $qN_1 \times qN_2$ where q is a magnification rate. For accelerating the simulated calculation, both artistic HR image and LR images are departed into the over-intersection miniature square structures as verified in fig.1(a) and fig.1(b) and, then, are restructured in ordered column-wise lexicographical vector form. Finally, for a stochastic impression of the MSRR problem formulation, the over-intersection miniature square structures of LR images is expounded as $\underline{Y}_k \in \mathbb{R}^{M^2}$ which have the measurement as $M^2 \times 1$ and the over-intersection miniature square structures of HR image is expounded as $\underline{X} \in \mathbb{R}^{q^2M^2}$ which have the measurement as $L^2 \times 1$ or $q^2M^2 \times 1$. Therefore, the over-intersection miniature square structures of HR image and LR images are stochastically signified as

$$\underline{Y}_k = D_k H_k F_{Tk} \underline{X} + \underline{V}_k \quad ; k = 1, 2, \ldots, N \qquad (1)$$

The matrix of an original inspected shifted motion between reference image and inspected image is expounded as F_{Tk} (where $F_{Tk} \in \mathbb{R}^{q^2M^2 \times q^2M^2}$) and the defocused matrix with both time invariant and space invariant is expounded as H_k (where $H_k \in \mathbb{R}^{q^2M^2 \times q^2M^2}$). The de-magnification rate matrix with a constant image is expounded as D_k (where $D_k \in \mathbb{R}^{M^2 \times q^2M^2}$) and the noise matrix from the inspected system is expounded as $\underline{V}_k$ (where $\underline{V}_k \in \mathbb{R}^{M^2}$). The original over-intersection miniature square structures of HR image and LR images are stochastically signified in fig.1(c).

2.2 The Video L1-L2 MSRR Scheme Established on Classical Registration

For L1 or L2 error function [2], we can stochastically signify the MSRR problem equation in the form of statistical optimization classis from integrating the ordinary Tikhonov prior function as

$$\underline{X} = \underset{\underline{X}}{\text{ArgMin}} \left\{ \sum_{k=1}^{N} \rho\left(D_k H_k F_{Tk} \underline{X} - \underline{Y}_k\right) + \lambda \cdot \left(\Gamma \underline{X}\right)^2 \right\} \qquad (2)$$

where $\rho(\cdot)$ is L1 or L2 error function, λ is the prior function parameter and Γ is the Tikhonov prior function where the Laplacian prior kernel can be easily signified as.

$$\Gamma_{\text{KERNEL}} = \tfrac{1}{8}\begin{bmatrix}1 & 1 & 1 & ; & 1 & -8 & 1 & ; & 1 & 1 & 1\end{bmatrix} \quad (3)$$

Using the 1st order minimization technique for example, the steepest descent technique [21], the MSRR solution from the above equation can be signified as

$$\underline{\hat{X}}_{n+1} = \underline{\hat{X}}_n + \beta \cdot \left\{ \begin{matrix} \left(\sum_{k=-N}^{N} F_{Tk}^T H_k^T D_k^T \psi\left(\underline{Y}_k - D_k H_k F_{Tk} \underline{\hat{X}}_n \right) \right) \\ -\left(\lambda \cdot \left(\Gamma^T \Gamma \right) \underline{\hat{X}}_n \right) \end{matrix} \right\} \quad (4)$$

where $\psi(\cdot) = \rho'(\cdot)$ and β is the calculated constant of the 1st order minimization technique.

3. The Proposed Video MSRR Scheme Established on a Universal Inspection Registration

In this section, the paper first presents the novel registration and the novel deformed matrix F_k. Later, this paper mathematically describes the algebraic formulation of MSRR problem by using the novel deformed matrix F_k. Finally, this paper mathematically explains the solution of this MSRR problem in both L1 and L2 error function.

3.1 The Universal Inspection Registration for MSRR Scheme

The proposed registration for universal inspected model of MSRR is based on a fast affine block-based transform [13]. The registration can be disentangled into 2 sub-processes. The first sub-process of this registration technique disentangles

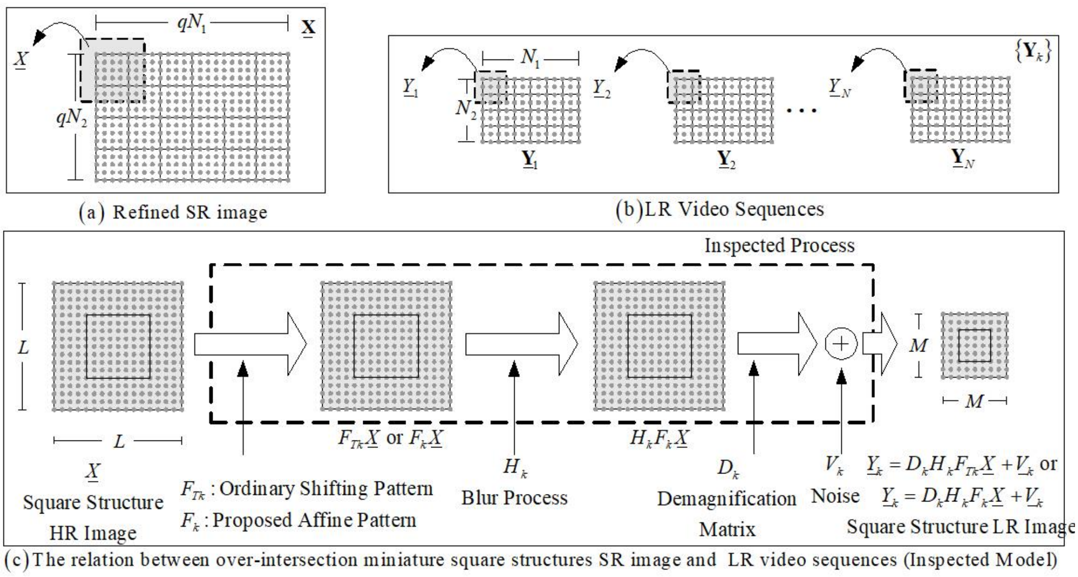

Figure 1 The universal inspection registration [15]

the whole image into many miniature square structures by divorcing both the inspected image and the reference image into 50% over intersection miniature square structure, which have the measurement as 16x16. The cardinal propose of the first sub-process is not only for disclosing and enumerating the regional moving but also for dwindling the enumerated time, especially when the parallel processing is implemented. The second sub-process enumerates the motion vector, which consists of six affine parameter, instead of two shifting parameter, between the inspected frame and the reference frame by using the M3SS (Modified Three Step Search) technique [13]. For dwindling the ultimately processing time of affine motion vector enumerating, the M3SS (Modified Three Step Search) technique is proposed. The M3SS, which is found on the famous 3SS of the ordinary shifting parameter estimation, is proposed to reduce a very high computational load in affine motion vector estimation. As a result, for each 7x7 inspecting square structures (inspected shifted motion) and $\pm 20^{O}$ degree (rotation, broadening or extrication inspecting pattern), the number of inspecting is $3^6 = 729$ (the motion vector is modified in 6 unknown affined parameters instead of 2 parameters) in the first inspecting process and, then, the group of modified affine parameters, which make the lowest error, is reused as the midpoint of the next inspecting process but the inspecting square structure is dwindled by half in the next inspecting process until the inspecting square structure is identical to pre-setting value. The parameter turning principle of M3SS in this article was found on the simulation results, which make the motion vector enumeration of the Foreman, Carphone and Stefan the highest PSNR [13], the number of inspecting is set to be 3.65E+3. Correlated with the ordinary shifting parameter estimation at ¼ subpixel level and 9x9 inspecting square structures, the number of inspecting of M3SS is higher than FS (Full Search) of the ordinary shifting parameter estimation about 3 enumerating times however the PSNR result from M3SS technique is ultimately higher than the PSNR result from ordinary technique about 5-6 dB. Finally, the motion vector from universal inspection registration is used to create the matrix of an inspected motion between a reference image and an inspected image or F_k in the same manner as the affine inspection registration [28].

3.2 The Universal Inspection Model for MSRR Scheme

For handling with a real or complex inter-frame motion pattern, the universal inspection registration [15], established on a fast affine block-based transform [13], was proposed in the form of an inspected shifted motion matrix $F_k \in \mathbb{R}^{q^2M^2 \times q^2M^2}$, which is nonisometric inter-frame deformation pattern such as affine motion pattern between over-intersection miniature square structures of HR image $\underline{X}$ and LR images $\underline{Y}_k$. Then, the over-intersection miniature square structures of HR image and LR images are stochastically signified

$$\underline{Y}_k = D_k H_k F_k \underline{X} + \underline{V}_k \quad ; k = 1, 2, \ldots, N \tag{5}$$

The universal inspected over-intersection miniature square structures of HR image and LR images are stochastically signified in fig.1(c).

3.3 The Video L1 MSRR Scheme Established on Universal Inspection Registration

In this division, the MSRR problem is first mathematically formulated under the stochastic maximum a posteriori framework and the universal inspection registration but the solution of this MSRR [17], which stochastically convinces the Eq.(1) or Eq.(2), in the case of under-determined situation has an infinite possible solutions because the problem of this MSRR is signified as ill-posed condition. Moreover, the solutions of this MSRR in the case of over-determined situation is unreliable because if there is the little noise from the inspected system will cause the dramatic different values of the solution thence Tikhonov prior function is generally required in the sense of the stochastic computation for enumerating the MSRR solution by getting rid of artifacts in the MSRR solution and by accelerating the convergent rate.

One of the most attractive error function for noise-vigorous perspective, which is generally undertaken in MSRR field [7-8,22], is L1 error function [2]. Thence, we can stochastically signify the MSRR problem equation in the form of statistical optimization classis from integrating the ordinary Tikhonov prior function as

$$\underline{X} = \underset{\underline{X}}{\text{ArgMin}}\left\{\sum_{k=1}^{N}\left\|D_k H_k F_k \underline{X} - \underline{Y}_k\right\| + \lambda\cdot\left(\Gamma \underline{X}\right)^2\right\} \quad (6)$$

Using the 1st order minimization technique for example, the steepest descent technique [21], the MSRR solution from the above equation can be signified as

$$\underline{\hat{X}}_{n+1} = \underline{\hat{X}}_n + \beta\cdot\left\{\begin{array}{l}\left(\sum_{k=-N}^{N} F_k^T H_k^T D_k^T \,\text{sign}\left(\underline{Y}_k - D_k H_k F_k \underline{\hat{X}}_n\right)\right)\\ -\left(\lambda\cdot\left(\Gamma^T\Gamma\right)\underline{\hat{X}}_n\right)\end{array}\right\} \quad (7)$$

where β is the calculated constant of the 1st order minimization technique.

3.4 The Video L2 MSRR Scheme Established on Universal Inspection Registration

Another of the most attractive error function for real implemented perspective, which is generally undertaken in MSRR field [22,29,3], is L2 error function. Thence, we can stochastically signify the MSRR problem equation in the form of statistical optimization classis from integrating the ordinary Tikhonov prior function as

$$\underline{X} = \underset{\underline{X}}{\text{ArgMin}}\left\{\sum_{k=1}^{N}\left\|D_k H_k F_k \underline{X} - \underline{Y}_k\right\|_2^2 + \lambda\cdot\left(\Gamma \underline{X}\right)^2\right\} \quad (8)$$

Using the 1st order minimization technique for example, the steepest descent technique [21], the MSRR solution from the above equation can be signified as

$$\underline{\hat{X}}_{n+1} = \underline{\hat{X}}_n + \beta\cdot\left\{\begin{array}{l}\sum_{k=1}^{N} F_k^T H_k^T D_k^T \left(\underline{Y}_k - D_k H_k F_k \underline{\hat{X}}_n\right)\\ -\left(\lambda\cdot\left(\Gamma^T\Gamma\right)\underline{\hat{X}}_n\right)\end{array}\right\} \quad (9)$$

4. The Results of Proposed Video MSRR Scheme

This partition proves the outperforming of the MSRR schemes with the proposed universal inspection registration by simulating under four noise models at several noise energy levels on Susie and Foreman, copious image products. This simulation is written by MATLAB program and the over-intersection miniature square structures of HR image and LR images are stochastically signified as 8x8 and 16x16, respectively.

The guideline [23, 7-8] of simulated parameter nomination in our simulation is to set the simulated parameters which generate the maximum PSNR and best envision desirable result. Furthermore, every simulation is reiterated a lot of times with dissimilar values and the maximum PSNR & the best envision desirable results are nominated.

4.1 The generation of LR images from original HR images

In this simulation, the original HR Susie (at 38, 39, 40, 41 and 42 frame) at 176x144 resolution for enhancing the refined SR image (40 frame of Susie) and Foreman (108, 109, 110, 111 and 112 frame) sequence for enhancing the refined SR image (110 frame of foreman) are used in this simulation because both sequences have complicated edge detail and complex inter-frame motion pattern therefore the number of LR images is five images or N=5 for using in each MSRR schemes as indicating in the following block diagram of generating of LR images from original HR images in fig.2. Each original images was defocused by both 3x3 time invariant and space invariant Gaussian filter is expounded as H_k and, then, was de-magnified by 2x2 to has 88x72 resolution and, then, was added by noise from the inspected system is expounded as $\underline{V}_k$.

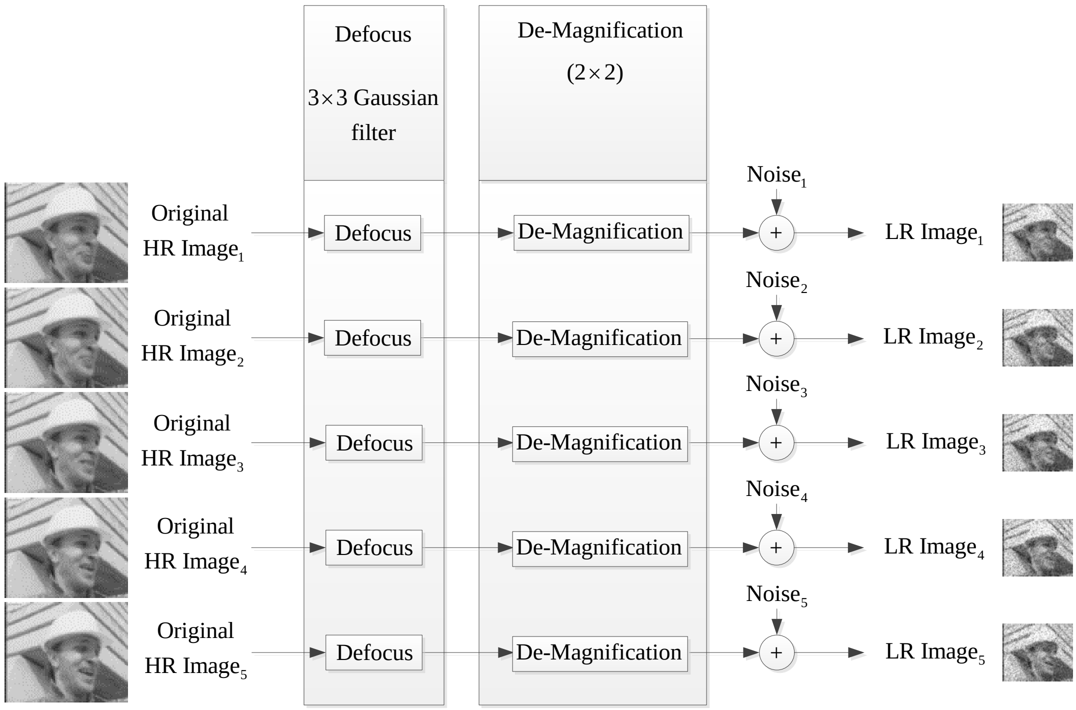

Figure 2 The block diagram of the generation of LR images from original HR images

The LR images are added by the following four noise models: additive Gaussian model, multiplicative Gaussian model, Poisson model and Impulsive model. Five noise energy levels are applied in additive Gaussian model and three level energy levels are applied in both multiplicative Gaussian model and impulsive model. One energy level of noise is applied in Poisson model. The detail of energy levels of noise model is as following:

1) Additive Gaussian model: PSNR of the noisy LR image = 25, 22.5, 20, 17.5, 15 dB

2) Multiplicative Gaussian model: V = 0.01, 0.02, 0.03.

3) Impulsive Model: noise density=0.5%, 1.0% and 1.5%

4.2 The Results of Proposed Video MSRR Scheme with the Universal Inspection Model

The PSNR results of the refined SR image (40 frame of Susie) and the refined SR image (110 frame of foreman) are summarized in Table 1 and Table 2 respectively.

Table 1 The comparative PSNR results of the refined SR image (40 frame of Susie) [15]

Noise Model	The PSNR of SRR Image (dB)				
	LR Image	L1 : Classic Model	L2 : Classic Model	L1 : Gen. Model	L2 : Gen. Model
AWGN (dB):					
SNR=25	25.8468	26.0369	25.8468	**26.1473**	25.8468
SNR=22.5	24.8508	25.4006	24.8508	**25.5834**	24.8508
SNR=20	23.7206	24.7384	23.7206	**24.9608**	24.0387
SNR=17.5	22.1395	24.8148	22.1395	**24.0890**	22.8283
SNR=15	20.3124	22.7614	20.3124	**23.1151**	21.1894
Poisson	25.0577	25.5626	25.0577	**25.7916**	25.1040
Salt&Pepper:					
D=0.005	25.5815	25.8052	25.5815	**25.9735**	25.5815
D=0.010	24.6287	25.1489	24.6287	**25.3920**	24.8303
D=0.015	23.6269	24.5757	23.6269	**24.8592**	24.2964
Speckle:					
V=0.01	23.7767	24.8022	23.7767	**25.0185**	24.1172
V=0.02	21.8538	23.7556	21.8538	**24.0958**	22.7284
V=0.03	20.5570	22.9761	20.5570	**23.3854**	21.7708

Table 2 The comparative PSNR results of the refined SR image (110 frame of foreman) [15]

Noise Model	The PSNR of SRR Image (dB)				
	LR Image	L1 : Classic Model	L2 : Classic Model	L1 : Gen. Model	L2 : Gen. Model
AWGN (dB):					
SNR=25	30.1487	30.3824	30.1487	**30.6615**	30.2347
SNR=22.5	29.0574	29.6625	29.0574	**30.0186**	29.4315
SNR=20	27.5740	28.8004	27.5740	**29.1304**	28.3754
SNR=17.5	25.7765	26.1635	25.7765	**28.0193**	27.0041
SNR=15	23.7393	26.2371	23.7393	**26.6879**	25.2707
Poisson	27.9892	28.8819	27.9892	**29.3107**	28.8507
Salt&Pepper:					
D=0.005	29.3506	29.7082	29.3506	**30.0868**	29.5284
D=0.010	27.3206	28.2861	27.3206	**28.7302**	27.8977
D=0.015	25.5210	27.0972	25.5210	**27.5187**	26.2784
Speckle:					
V=0.01	27.5301	28.6916	27.5301	**29.1562**	28.3942
V=0.02	25.2720	27.2486	25.2720	**27.7187**	26.6633
V=0.03	23.9860	26.7384	23.9860	**27.0925**	25.5199

The results of the refined SR images that are based enumerated by the L1 MSRR scheme established on universal inspection model, which can be simulated by Eq. (7), and L2 MSRR scheme established on universal inspection model, which can be simulated by Eq. (9) analogously shows with L1 and L2 MSRR scheme established on originally inspection model, which can be simulated from the result of Eq. (4).

From the results in Table 1 (40 frame of Susie) and Table 2 (110 frame of foreman), we can deduce as follow:

From the inspected registration prospective, the MSRR scheme with the proposed inspected registration has the better PSNR than MSRR scheme with the original inspected registration.

From the error function prospective, the MSRR scheme with L1 error function has the better PSNR than MSRR scheme with L2 error function for the original inspected registration and the proposed inspected registration, respectively because the L2 error function is more problematic the noise from the inspected system or registration error than L1 error function.

From the overall prospective, the MSRR scheme with L1 error function and the proposed inspected registration has the best PSNR than other MSRR schemes.

From the overall prospective, the MSRR scheme with L2 error function and the original inspected registration cannot enhance the PSNR because L2 error function is more problematic for the severe error from the original inspected registration.

The envision desirable results of the refined SR image (for 40 frame of Susie) and the refined SR image (for 110 frame of Foreman) from the proposed video MSRR scheme is indicated in figure 3 and figure 4, respectively.

Considering Additive Gaussian model of the noisy LR images at 25, 22.5, 20, 17.5, 15 dB, the envision results is indicated in figure 3(a) – 3(e) for the refined SR image (for 40 frame of Susie) and in figure 4(a) – 4(e) for the refined SR image (for 110 frame of Foreman), respectively.

Considering Poisson model of the noisy LR image, the envision results is indicated in figure 3(f) for the refined SR image (for 40 frame of Susie) and in figure 4(f) for the refined SR image (for 110 frame of Foreman), respectively.

Considering Impulsive model of the noisy LR image at noise density=0.5%, 1.0% and 1.5%, the envision results is indicated in figure 3(g) – 3(i) for the refined SR image (for 40 frame of Susie) and in figure 4(g) – 4(i) for the refined SR image (for 110 frame of Foreman), respectively.

Considering Multiplicative Gaussian model of the noisy LR images at V=0.01, V=0.02 and V=0.03, the envision results is indicated in figure 3(j) – 3(l) for the refined SR image (for 40 frame of Susie) and in figure 3(j) – 3(l) for the refined SR image (for 110 frame of Foreman), respectively.

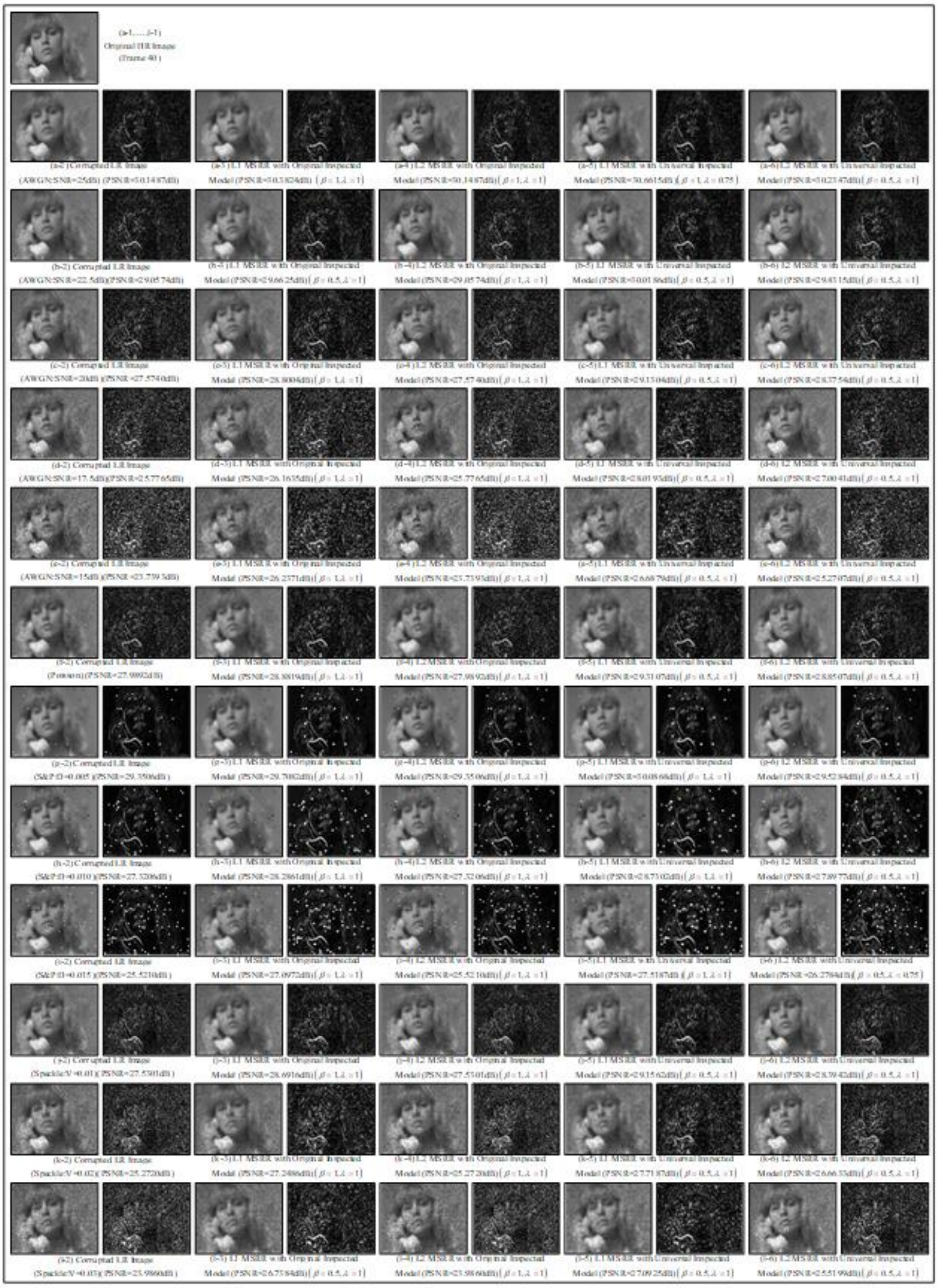

Figure 3 The envision desirable results of the refined SR images (for 40 frame of Susie)

(In each refined SR images, the right-side image of each sub-image is the total distinction, which is magnified by five, between the refined SR image (at left-size image) and the artistic image)

Figure 4 The envision desirable results of the refined SR images (for 110 frame of Foreman)

(In each refined SR images, the right-side image of each sub-image is the total distinction, which is magnified by five, between the refined SR image (at left-size image) and the artistic image) [15]

5. The Discussion and Summary

The universal inspected model, which is desired for applying on video MSRR scheme established on both L1 and L2 error function, is proposed. Thence, the video MSRR scheme with this universal inspected model can be imposed on the real standard video with the complicated motion pattern. The results from the simulation obviously convey that the proposed universal inspected model can be imposed on the real standard video with outperforming PSNR results and envision results from the video MSRR scheme.

For the future research, this proposed universal inspected model is mathematically combined with the powerful adaptive robust error function [24] (instead of L1 and L2 error function) for applying on the real noisy videos.

Portions of this research work were presented at the IEEE-ISPACS-2008 Conference, 8-11 Dec 2008 as "General Observation Model for an Iterative Multiframe Regularized Super-Resolution Reconstruction for Video Enhancement" [15].

6. Acknowledgement

The research project was funded by Assumption University.

7. References

[1]. Altunbasak, Y., Patti, A. J., & Mersereau, R. M. (2002). Super-resolution still and video reconstruction from MPEG-coded video. IEEE Transactions on Circuits and Systems for Video Technology 12(4), 217-226.

[2]. Black, M. J., Sapiro, G., Marimont, D., & Heeger, D. (1998). Robust anisotropic diffusion. IEEE Transactions on Image Processing 7(3), 421-432.

[3]. Elad, M., & Feuer, A. (1997). Restoration of a single superresolution image from several blurred, noisy, and undersampled measured images. IEEE Transactions on Image Processing 6(12), 1646-1658.

[4]. Elad, M., & Feuer, A. (1999a). Superresolution restoration of an image sequence: adaptive filtering approach. IEEE Transactions on Image Processing 8(3), 387-395. DOI: 10.1109/83.748893

[5]. Elad, M., & Feuer, A. (1999b). Super-resolution reconstruction of image sequences. IEEE Transactions on Pattern Analysis and Machine Intelligence 21(9), 817-834. DOI: 10.1109/34.790425

[6]. Elad, M., & Hel-Or, Y. (2001). A fast super-resolution reconstruction algorithm for pure translational motion and common space-invariant blur. IEEE Transactions on Image Processing 10(8), 1187-1193.

[7]. Farsiu, S., Robinson, M. D., Elad, M., & Milanfar, P. (2004). Fast and robust multiframe super resolution. IEEE Transactions on Image Processing 13(10), 1327-1344. DOI: 10.1109/TIP.2004.834669

[8]. Farsiu, S., Elad, M., & Milanfar, P. (2006). Multiframe demosaicing and super-resolution of color images. IEEE Trans. on Image Processing 15(1), 141-159.

[9]. He, Y., Yap, K.-H., Chen, L. and Pui, L. (2007). A Nonlinear Least Square Technique for Simultaneous Image Registration and Super-Resolution. IEEE Trans. on Image Processing 16(11). 2830-2841.

[10]. Ng, M. K., & Bose, N. K. (2003). Mathematical analysis of super-resolution methodology. IEEE Signal Processing Magazine 20(3), 62-74.

[11]. Kang, M. G., & Chaudhuri, S. (2003). Super-resolution image reconstruction. IEEE Signal Processing Magazine 20(3), 19-20.

[12]. Park, S. C., Park, M. K., & Kang, M. G. (2003). Super-resolution image reconstruction: a technical overview. IEEE Signal Processing Magazine 20(3), 21-36. DOI: 10.1109/MSP.2003.1203207

[13]. Patanavijit, V. & Jitapunkul, S. (2006). A Modified Three-Step Search Algorithm for Fast Affine Block Base Motion Estimation. Proceeding of International Workshop on Advanced Image Technology 2006 (IWAIT 2006), Okinawa, Japan, Jan. 2006.

[14]. Patanavijit, V. (2008). Andrew's Sine estimation for a robust iterative multiframe super-resolution reconstruction using stochastic regularization technique. Proceeding of IEEE Northeast Workshop on Circuits And Systems (IEEE-NEWCAS-TAISA'08), Montreal, Canada, June 2008.

[15]. Patanavijit, V. & Jitapunkul, S. (2008). General Observation Model for an Iterative Multiframe Regularized Super-Resolution Reconstruction for Video Enhancement. Proceeding of IEEE International Symposium on Intelligent Signal Processing and Communication Systems (ISPACS 2008), Bangkok, Thailand, Feb. 2009.

[16]. Patanavijit, V. (2009a). Super-resolution reconstruction and its future research direction, AU Journal of Technology (AU J.T.), Assumption University of Thailand, Bangkok, Thailand, Jan. 12(3), 149–163.

[17]. Patanavijit, V. (2009b). Mathematical analysis of stochastic regularization approach for super-resolution reconstruction, AU Journal of Technology (AU J.T.), Assumption University of Thailand, Bangkok, Thailand, April. 12(4), 235–244.

[18]. Patanavijit, V. (2009c), A robust iterative multiframe SRR based on Andrew's Sine stochastice with Andrew's Sine-Tikhonov regularization, Proceeding of IEEE International Symposium on Intelligent Signal Processing and Communication Systems (ISPACS 2008), Bangkok, Thailand, 8-11 Feb. 2009. Page(s): 1-4. DOI: 10.1109/ISPACS.2009.4806736

[19]. Patanavijit, V. (2009d), Video enhancement using a robust iterative SRR based on Andrew's Sine regularization technique,

Proceeding of IEEE International Symposium on Intelligent Signal Processing and Communication Systems (ISPACS 2009), Kanazawa, Japan, 2009. Page(s): 115-118.

[20]. Patanavijit, V. (2011), A robust recursive SRR based on Andrew's Sine stochastic estimation with fast affine block-based registration for video enhancement, Proceeding of The 34th Electrical Engineering Conference (EECON-34), Ambassador City Jomtien Hotel, Pataya, Chonburi, Thailand, Dec.

[21]. Patanavijit, Vorapoj (2013), Computational Tutorial of Steepest Descent Method and Its Implementation in Digital Image Processing, ECTI E-magazine, ECTI Association, Bangkok, Thailand, Vol. 7, No. 1, Jan. – Mar. (http://www.ecti-thailand.org/emagazine/)

[22]. Patanavijit, V. (2015). Comparative experimental exploration of robust norm functions for iterative super resolution reconstructions under noise surrounding, ECTI Transactions on EEC (Electrical Engineering/ Electronics and Communications), 13(2), 83-91. ECTI Association, Thailand.

[23]. Patanavijit, V. & Thakulsukanant K. (2016). A Performance Impact of Andrew's Sine Threshold for a Robust Regularized SRR Based on ML Framework, Rangsit Journal of Arts and Sciences, Rangsit University, Vol. 6 No. 1, January-June 2016. (ISSN 2229-063X (Print)/ISSN 2392-554X (Online))

[24]. Patanavijit, V. (2015), Comparative Experimental Exploration of Robust Norm Functions for Iterative Super Resolution Reconstructions under Noise Surrounding, ECTI Transactions on EEC (Electrical Engineering/Electronics and Communications), ECTI Association, Thailand. Vol.13, No.2, August 2015. (ISSN 1685-9545)

[25]. Patti, A. J., & Altunbasak, Y. (2001). Artifact reduction for set theoretic super resolution image reconstruction with edge constraints and higher-order interpolation. IEEE Transactions on Image Processing 10(1), 179-186.

[26]. Rajan, D., Chaudhuri, S., & Joshi, M. V. (2003). Multi-objective super resolution concepts and examples. IEEE Signal Processing Magazine 20(3), 49-61.

[27]. Rajan, D., & Chaudhuri, S. (2003). Simultaneous estimation of super-resolution scene and depth map from low resolution defocuses observations. IEEE Transactions on Pattern Analysis and Machine Intelligence 25(9), 1102-1117.

[28]. Rochefort, G., Champagnat, F., Besnerais, G. L. & Giovannelli, Jean-Francois (2006). An Improved Observation Model for Super-Resolution Under Affine Motion. IEEE

Transactions on Image Processing 15(11), 3325-3337.

[29]. Schultz, R. R., & Stevenson, R. L. (1996). Extraction of high-resolution frames from video sequences. IEEE Transactions on Image Processing 5(6), 996-1011.

[30]. Patanavijit, V. (2016), Mathematical Tutorial of Discrete-Time Analysis of Sampling Rate Changing Concept for Digital Signal Processing and Digital Communication Prospective, RMUTT Journal Sciences and Technology, RMUTT, Vol. 6, No.2, July.-Dec. 2016.

[31]. Tungkasthan, A., Efficient ACC using Binary Coding Stream for Color Descriptor, Engineering Journal Siam University, Vol. 33, 2016.